Numerical Methods in Civil Engineering

Liquefied Residual Strength of Undrained Sand upon A Parametric Approach to Hypo-elastic Model

Farzad Peyman[*] , Seyed Amirodin Sadrnejad[**]

ARTICLE INFO

Article history:
Received:
January 2017.
Revised:
April 2017.
Accepted:
July 2017

Keywords:
hypo-elastic model,
sand,
drained,
undrained,
liquefaction.

Abstract:

A parametric study approach evaluating drained/undrained behavior of sand has been developed as a simple/quick hypo-elastic model capable of being used in engineering applications. The volumetric interaction of sand grains behavior against pore water pressure induces the tendency of soil mass volume change to contract/dilate due to variation of effective mean stress on solid grain, pore water pressure by compressibility and shear induced dilation/compression which lead to an ideal condition for constant total volume of undrained test. However, any individual volume changes of named components may result in a partial reduction of the effective mean stress to an extent that can be disclosed as a local decrease in stress deviator. In the extreme case, the effective stress components may become so small (or even zero) resulting in complete loss of strength and cause the soil to flow in a manner resembling a liquid known as liquefaction of sand. However, in real case, any possibility of water dissipation or volumetric change tendency of components can change the state/condition to activate some shear strength by increasing the effective mean stress.

The proposed parametric study approach is able to present such volumetric variation condition leading to partial or complete liquefaction condition. This model has predicted and verified several compression triaxial test results of sands. The verification of model is presented by comparing the obtained results with the experimental result of Nevada sand, in both drained and undrained conditions. The proposed model can be successfully used for other soils behavior by using the proposed parametric study method including the required parameters to achieve acceptable results.

1. Introduction

The assessment of mobilized internal friction in non-cohesive undrained soil and observation of physical model of different tests has significantly revealed our knowledge of soil grains internal mechanisms associated with liquefaction. Results from several soil experiments have generated a large database for calibration/verification of computational models. Computationally, significant advances have also taken place and reveal that plenty of characteristics parameters affect soil behavior, while very few of them can be handled in most of developed constitutive models in engineering.

** Phd Student, Department of Civil Engineering, College of Engineering, Tehran Science and Research Branch, Islamic Azad University, Tehran, Iran. E-mail: f.peyman@srbiau.ac.ir*

***Corresponding author, Prof. of Civil Eng.Dept, K.N.Toosi University of Tech., Tehran, Iran. E-mail: sadrnejad@kntu.ac.ir*

For instance, the concept of state-dependent dilatancy into sand constitutive modeling (Manzari and Dafalias, 1997 [9], Li and Dafalias, 2000 [7]) tried to allow for a unified treatment of sand behavior at different relative densities with a single set of model constants. Despite the great progress in both physical and numerical modeling of liquefaction, a small number of developed models are able to cope with inter granular volumetric interactions with the development of pore water pressure in partly or fully liquefied saturated soils (Been, 1999 [4]).

Although, many mathematical models developed for predicting soil behavior have been represented in equations (Ling and Yang, 2006 [8], Monkul and Yamamuro, 2011 [10] , Nova and Wood, 1979 [12], Olivera Bonilla 2004 [13], Paster *et al*., 1990 [14], Shahir *et al*., 2012 [18], Wan and Guo, 2001 [21], Yin *et al*., 2014 [22], Zienkiewicz, 1984 [23]) with regards to vast soil diversity in aggregation,

[DOR: 20.1001.1.23454296.2017.2.1.5.4]

[DOI: 10.29252/nmce.2.1.49]

aggregate materials, fabric, non-homogeneity of permeability, atmospheric conditions, applied stress conditions, and so on, most of these models are unable to represent all of the characteristics of soils behavior features completely during liquefaction. In general, the use of these models to provide accurate results is somehow difficult with regards to several complex parameters and may be not acceptable to apply them in industry (Lee and Seed, 1967 [6], Monkul, 2010 [11]).

In modeling points of view, we require more knowledge about mechanical and physical grains motion features and representing correct dominant mathematic terms in order to understand the aspects of hidden and concealed facts of materials behavior. However, lack of knowledge about these facts results in inaccuracies in problem analysis, which in turn results in unsafe and uneconomical designing. In spite of the wonders of mechanical behavior of materials, we have yet to find appropriate principles to overcome our lack of knowledge of microscopic and macroscopic materials. These principles are mostly neither general nor comprehensive, and in some cases, compels one to take some steps to modify them with combination, separation, and generalization. For this matter, soils have various and complex behaviors which inexactitude in estimating their behavior in certain cases, in particular soil inter-granular interaction with pore water pressure. With similar point of view, at the beginning of some phenomena for examples hydraulic fracture, liquefaction, and slope slipping is calm and safe, despite that, a small fracture could easily lead to massive damages .Therefore, the behavior of soils in this case should be studied and investigated with more precision and care, and more accurate micro level models should be represented. Also, more care and attention must be paid to parametric evaluation method. Consequently, applying more precise and simple models with appropriate parameter values leads to more economical design, as well as providing safety for soil made structures, regions and people (RAHMAN *et al*., 2010 [15], Roscoe *et al*., 1958 [16], Sasiharan, 2006 [17]).

In this paper, it is tried efforts have been made to introduce implicit method, applicable in engineering model in the form of hypo-elastic form with parametric study for quick estimate of both drained and saturated granular soils with capability to examine/of examining both hardening and softening behavior. This model is obtained upon a parametric approach by investigation on parameter variations in several compression triaxial tests results on Nevada sands, in both drained and undrained conditions (Arulanandan *et al*., 1995 [1], Arulmori *et al*., 1992 [2], Ling and Yang, 2006 [8], Shahir *et al*., 2012 [18]).

With regards to reality of all aspects of soil behavior which depend on infinite number of parameters, each may affect and respond to one or even several aspects. However, while a few limited numbers of parameters are defined for a model, it means that each parameter must cover and represent the effects of many of those infinite number responsibilities within a certain limited domain, otherwise this parameter has to vary and it cannot be assumed constant. Accordingly, the use of simple model followed by limited number of parameters which is obtained through simple calibration of model with properly selected test results presenting the reality of such complex material behavior can be introduced as an applicable, rationalized and justified method in engineering.

Therefore, a parametric-based approach method proposed for assigning drained/undrained sand behavior leads to predicting deformability and stress distribution in soil. This approach is derived upon total stress change procedure to assess either drained or undrained leads to both partially or fully liquefied soil domain. Analyses are performed in the laboratory domain results, allowing the imposed earthquake motion to affect both the triggering and post-liquefaction deformations (Ishihara, 1996 [5], Vaid *et al*., 1990 [19], Verdugo and Ishihara, 1996 [20]).

2. Hypo-elasticity model for drained condition:

Starting with simple, ordinary compression drained triaxial test on sand, with specific initial void ratio and relative density, which is consolidated under confining pressure followed by increasing vertical stress, created/resulted in deviatoric stress and continued to rupture. In this case, soil volume would change and pore water pressure is equal to zero through load incements, and it can be written as follows (Atkinson and Bransby, 1977 [3]):

$$q = q' = \sigma_1 - \sigma_3 = \sigma'_1 - \sigma'_3 \tag{1}$$

$$p = p' = \frac{1}{3}(\sigma_1 + 2\sigma_3) = \frac{1}{3}(\sigma'_1 + 2\sigma'_3) \tag{2}$$

In these Eqs. :

q' = Deviatoric stress

p' = Mean effective stress

σ'_3 = Minor principal effective stress

σ'_1 = Major principal effective stress

During the first few stages of load increments sample behavior can be assumed as isotropic linear elastic and the stress-strain relations are written as follows:

$$q_i = q'_i = \sigma'_{1i} - \sigma'_{3i} = \frac{E_i}{1+\nu_i} \cdot (\varepsilon_{1i} - \varepsilon_{3i}) = E_i \cdot \varepsilon_{1i} \tag{3}$$

$$\nu_i = -\frac{\varepsilon_{3i}}{\varepsilon_{1i}} \tag{4}$$

$$p_i = p'_i = \frac{1}{3}(\sigma'_{1i} + 2\sigma'_{3i}) = \frac{1}{3} \cdot \frac{E_i}{1-2\nu_i} \cdot \varepsilon_{vi} \tag{5}$$

$$\varepsilon_{vi} = \varepsilon_{1i} + 2\varepsilon_{3i} = (1-2\nu_i) \cdot \varepsilon_{1i} \tag{6}$$

$$\frac{q'_i}{p'_i} = 3 \tag{7}$$

In these Eqs.:

q'_i = Deviatoric stress in every increment

p'_i = Mean effective stress in every increment

σ'_{3i} = Minor principal effective stress in every increment

σ'_{1i} = Major principal effective stress in every increment

ε_{3i} = Lateral strain in every increment

ε_{1i} = Axial strain in every increment

E_i = Elasticity coefficient in every increment

ν_i = Poisson's ratio in every increment

ε_{vi} = Volumetric strain in every increment

The normalized curves for Nevada sand in drained compression triaxial tests upon the use of initial parameters which are given in Table 1 (Arulanandan *et al*., 1995 [1],

[DOR: 20.1001.1.23454296.2017.2.1.5.4]

[DOI: 10.29252/nmce.2.1.49]

Arulmori *et al*., 1992 [2], Ling and Yang, 2006 [8], Shahir *et al*., 2012 [18]) are shown in Fig. 1.

Table 1: Characteristics of Nevada sand and the values of normalizing coefficient α for six sand samples in drained triaxial experiments (Arulanandan *et al*., 1995 [1], Arulmori *et al*., 1992 [2], Ling and Yang, 2006 [8], Shahir *et al*., 2012 [18])

Test	e_0	p'_0 *(kPa)*	***Dr*** *(%)*	α
1	0.728	40	42.4	1.000
2	0.726	80	43.0	1.001
3	0.718	160	45.0	1.005
4	0.657	40	61.2	1.035
5	0.652	80	62.5	1.037
6	0.651	160	62.8	1.038

The N and α values are defined as follows:

$$N = log\left(\frac{p'_{0i}\cdot\varepsilon_{1i}(\%)}{p'_i}\right) \quad (8)$$

$$\alpha = \left(\frac{e_{0(Dr=40\%)}}{e_{0(Dr=60\%)}}\right)^{\frac{1}{3}} \quad (9)$$

Where:

$e_{0(Dr=40\%)}$ = Initial void ratio of Nevada sand related to relative density 40%

$e_{0(Dr=60\%)}$ = Initial void ratio of Nevada sand related to relative density 60%

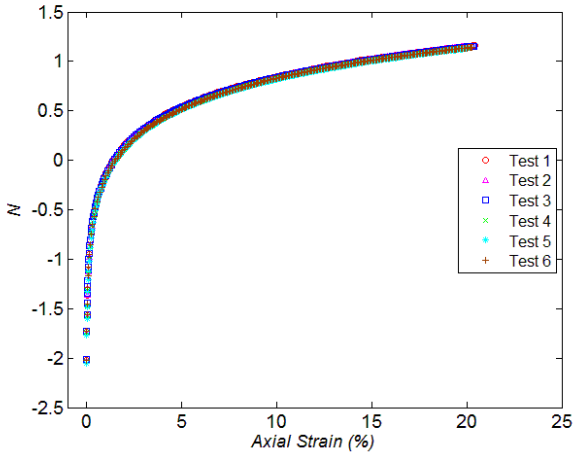

(a)

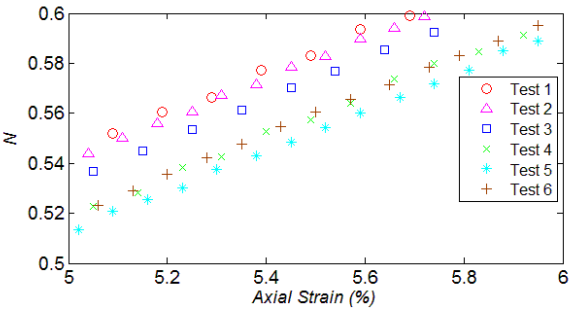

(b)

Fig. 1: Normalized curves for Nevada sand in drained triaxial tests. **(a)** *N:*ε_1 *(0-25% strain domain)* **(b)** *N:*ε_1 *(5-6% strain domain)*

The values of normalizing coefficient α for Nevada sand samples are calculated in Table 1.

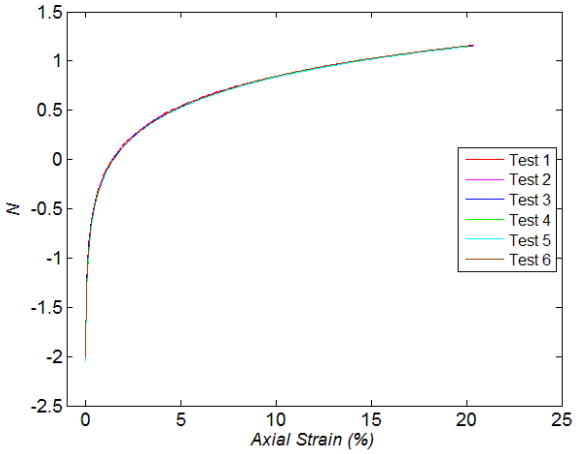

Fig. 2: More normalized curves for Nevada sand samples in drained triaxial tests

The N value is defined as follows:

$$N = log\left(\alpha\cdot\frac{p'_{0i}\cdot\varepsilon_{1i}(\%)}{p'_i}\right) \quad (10)$$

The normalized curves in the form of mathematical terms are presented as follows:

$$N = log\left(\alpha\cdot\frac{p'_{0i}\cdot\varepsilon_{1i}(\%)}{p'_i}\right) = f(\varepsilon_{1i}) = A(\varepsilon_{1i}(\%))^B + C \quad (11)$$

f is a function of ε_{1i} which presents the mathematical effects in hypo-elastic strain in drained test.

Constant coefficients A, B, and C are obtained calibration of model with experimental results as shown in Fig. 2. These values for Nevada sand are: A= *16.72*, B= *0.02515*, and C=-*16.88*.

The effects of parameter f on E_i is revealed by implementing Eq. (7) and (3) in Eq. (9). The result is written as follows:

$$E_i = 300\,p'_0\left(\frac{\alpha}{10^{f(\varepsilon_{1i}\%)}} - \frac{1}{\varepsilon_{1i}(\%)}\right) \quad (12)$$

Eq. (12) and (4) provide elastic parameters of sand behavior which must be updated in every increment of loading. This variation in fact, represents nonlinearity of drained sand behavior obtained through Eq. (3) and (5). Also, this application can present the nonlinear volumetric strain versus axial strain in every stress increment. Therefore, variation of ε_{vi} can be calculated as follow:

$$\varepsilon_{vi} = a\cdot(\varepsilon_{1i}\%)^b + c\cdot tanh(d\cdot\varepsilon_{1i}\%) \quad (13)$$

The values of parameters a, b, c, d, are found by calibration, as presented for Nevada sand in Table 2.

Table 2: The parameter values in Eq. (13) for Nevada sand

Test	***a***	***b***	***c***	***d***
1	0.1118	0.2664	-3.895	0.07802
2	0.1092	0.3132	-3.892	0.07504
3	0.1364	0.2700	-4.276	0.08175
4	0.1161	0.1241	-6.268	0.10930
5	0.1364	0.2192	-6.301	0.09929
6	0.2791	0.2135	-6.336	0.11140

[DOR: 20.1001.1.23454296.2017.2.1.5.4]
[DOI: 10.29252/nmce.2.1.49]

The parameter values presented in Table 2 which were found by calibrating of volumetric strain versus axial stress (Figs. 3a-c. and 4a-c.) are implemented in Eqs. (3) and (5), to present nonlinear behavior of undrained sand.

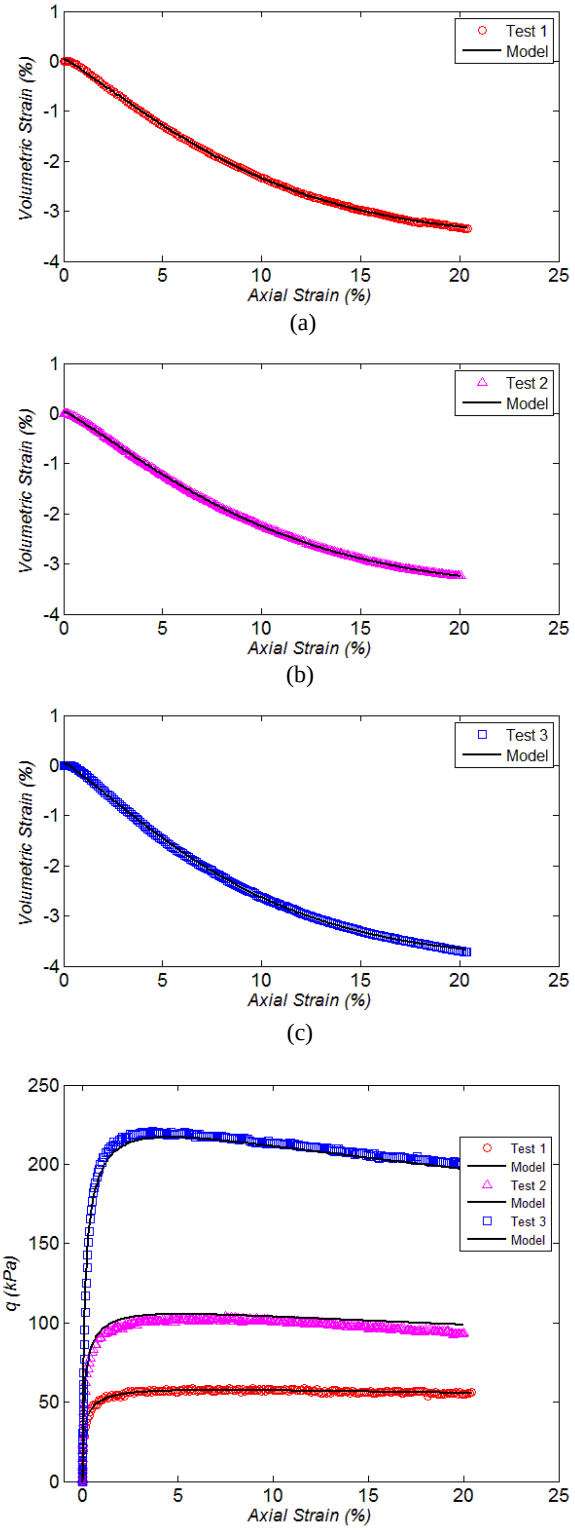

Fig. 3: The comparison model and drained tests, number 1, 2, and 3 (Nevada sand), **(a)** test 1, **(b)** test 2, and **(c)** test 3: ε_v-ε_1 , **(d)** q'-ε_1 tests 1, 2, and 3

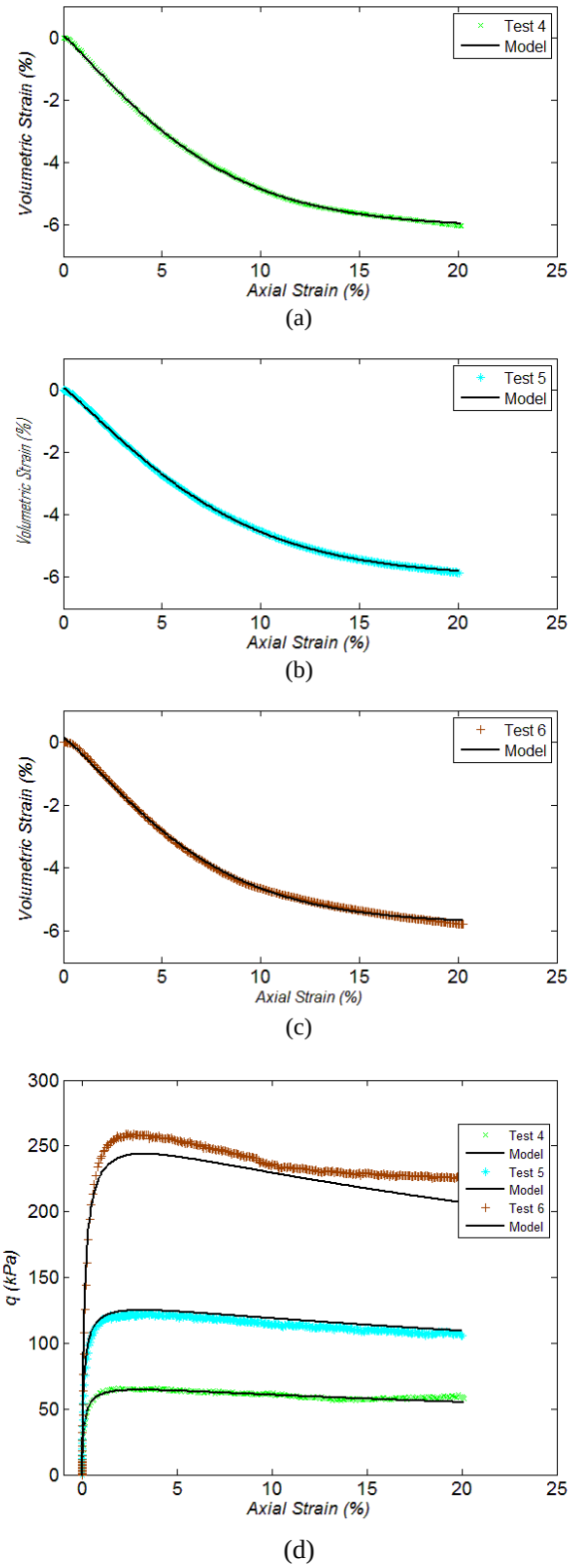

Fig. 4: The comparison between behavioral curves of drained experiments number 4, 5, and 6 on Nevada sand and the behavioral model. **(a),(b),(c)** ε_v-ε_1 , **(d)** q'-ε_1

The comparison of model results with experiments (Arulanandan *et al.*, 1995 [1], Arulmori *et al.*, 1992 [2], Ling and Yang, 2006 [8], Shahir *et al.*, 2012 [18]) as ε_v-ε_1 and q'-ε_1 are shown in Fig. 3 and 4. The high accuracy of model results reveals the capability of proposed model.

[DOR: 20.1001.1.23454296.2017.2.1.5.4]
[DOI: 10.29252/nmce.2.1.49]

3. Hypo-elastic Strain under undrained condition

In undrained compression triaxial test on sand, with specific initial void ratio and relative density, at first stage is consolidated under confining pressure without excess pore water pressure, followed by increasing the vertical stress creating deviatoric stress under undrained condition, it continued to rupture.

In this case, soil volume is constant and pore water pressure increases, therefore, the relations can be written as follows (Atkinson and Bransby, 1977 [3]):

$$q = q' = \sigma_1 - \sigma_3 = \sigma'_1 - \sigma'_3 \quad (14)$$

$$p' = \frac{1}{3}(\sigma'_1 + 2\sigma'_3) \quad (15)$$

$$p = \frac{1}{3}(\sigma_1 + 2\sigma_3) = p' + u \quad (16)$$

$$q_i = q'_i = \sigma'_{1i} - \sigma'_{3i} = E_i \cdot \varepsilon_{1i} \quad (17)$$

$$p'_i = \frac{q'_i}{3} + p'_0 - u_i \quad (18)$$

u = pore water pressure.

The parameter values of Nevada sand for undrained tests are given in Table 3, (Arulanandan *et al*., 1995 [1], Arulmori *et al*., 1992 [2], Ling and Yang, 2006 [8], Shahir *et al*., 2012 [18]) and similar to drained test case, the provided normalized curves are shown in Fig. 5.

Also, Table 3 presents initial values of parameters.

The N value is defined as follows:

$$N = log\left(\frac{E_i}{p'_i}\right) \quad (19)$$

$$N = log\left(\frac{E_i}{p'_i}\right) = f(\varepsilon_{1i}) = A(\varepsilon_{1i}(\%))^B + C \quad (20)$$

f is a function of ε_{1i} which implements the mathematical effects of strain on the given hypo-elastic behavior in the nonlinear behavior of undrained sand.

Constant coefficients A, B, and C are obtained through test results as shown in Fig. 5e. For Nevada sand the three parameters are: A= *-3.109*, B= *0.1166*, and C=*5.203*.

The combination of two Eqs. (18) and (20), could also conclude that:

$$E_i = \frac{10^{f(\varepsilon_{1i}\%)}(p'_0 - u_i)}{1 - 10^{f(\varepsilon_{1i}\%)} \cdot \frac{\varepsilon_{1i}(\%)}{300}} \quad (21)$$

E_i in Eq. (21) presents the variation of elastic modulus of sand for nonlinear behavior of undrained sand. The proposed nonlinearity could be effectively used to calculate u_i as follow:

$$u_i = \begin{cases} a' \cdot (\varepsilon_{1i}\%)^{b'} + c' \cdot tanh(d' \cdot \varepsilon_{1i}\%) & \varepsilon_{1i}\% \le \beta \\ e' \cdot \varepsilon_{1i}\% + f' & \varepsilon_{1i}\% \ge \beta \end{cases} \quad (22)$$

In this Eq. :

a', b', c', d', e', f', are practical measurable parameters which can be evaluated through calibration of model with test results.

The values of these parameters for Nevada sand are given in Table 4. Furthermore, the value of β can be obtained by the position of intersection point of the two presented terms in Eq. (22).

To show the capability of proposed model in predicting pore water pressure, upon coefficient values shown in Table 5, the variation of pore water pressure versus axial stress in undrained tests number 1 to 17 (Nevada sand) are compared with model as shown in Figs. 6-a to 15-a, respectively. The comparison of presented results with experiments reveals the capability of proposed model in prediction of pore water pressure variation in undrained tests well.

Table 3: Nevada sand samples characteristics in undrained triaxial tests (Arulanandan *et al*., 1995 [1], Arulmori *et al*., 1992 [2], Ling and Yang, 2006 [8], Shahir *et al*., 2012 [18])

Test	***e₀***	***p'₀ (kPa)***	***Dr (%)***
1	0.736	40	40.2
2	0.733	40	41.1
3	0.729	80	42.2
4	0.732	80	41.4
5	0.732	160	41.5
6	0.725	160	43.1
7	0.726	160	42.9
8	0.688	80	53.0
9	0.692	160	52.0
10	0.682	160	54.5
11	0.656	40	61.4
12	0.660	40	60.4
13	0.663	80	59.6
14	0.657	80	61.3
15	0.649	160	63.4
16	0.637	40	73.1
17	0.635	80	67.1

Figs. 6 to 15 represent a certain comparison of the model results with tests on Nevada sand. Accordingly, it is concluded that the Eq. 20 in proposed model is able to satisfy accurately the presented predictions upon three auxiliary parameters in model.

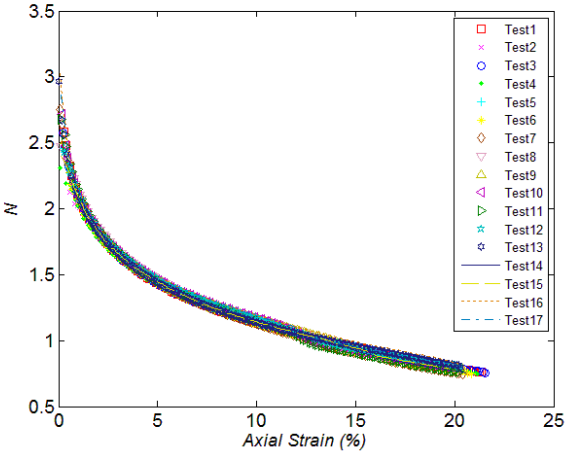

(a)

[DOR: 20.1001.1.23454296.2017.2.1.5.4]
[DOI: 10.29252/nmce.2.1.49]

[DOR: 20.1001.1.23454296.2017.2.1.5.4]

[DOI: 10.29252/nmce.2.1.49]

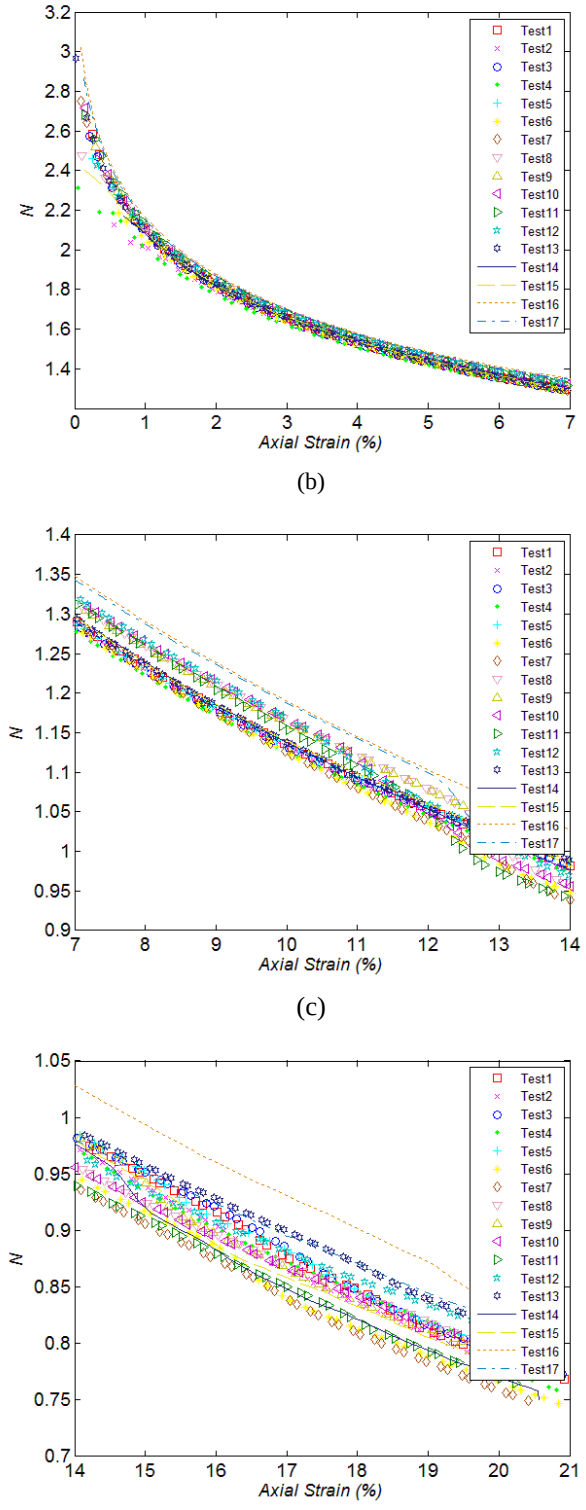

(b)

(c)

(d)

Fig. 5: Nevada sand samples normalized curves in undrained triaxial tests.
(a) *N:*ε_1 *(0-25% strain domain)*
(b) *N:*ε_1 *(0-7%) strain domain*
(c) *N:*ε_1 *(7-14% strain domain)*
(d) *N:*ε_1 *(14-21% strain domain)*

Table 4: Empirical coefficients for Eq. (22) for Nevada sand.

Test	*a'*	*b'*	*c'*	*d'*	*e'*	*f'*	*β*
1,2	164.7	0.8279	-4531	0.03303	1.975	-631.9	17.43
3,4	266.1	0.8209	-5646	0.04099	1.083	-712.3	18.23
5,6,7	283.6	0.7208	-3358	0.07472	3.017	-763.0	14.40
8	343.7	0.8340	-7071	0.04286	-4.946	-651.4	15.37
9,10	273.1	0.5340	-2225	0.08566	1.724	-767.6	14.43
11,12	386.7	0.7584	-4329	0.08383	0.682	-754.0	9.97
13,14	333.6	0.6801	-2920	0.11080	0.993	-742.4	8.99
15	743.6	0.8234	-8195	0.08640	0.571	-752.0	7.16
16	792.3	0.8654	-8999	0.08999	-1.325	-719.9	6.42
17	677.3	0.8278	-7757	0.08680	-0.192	-755.1	6.30

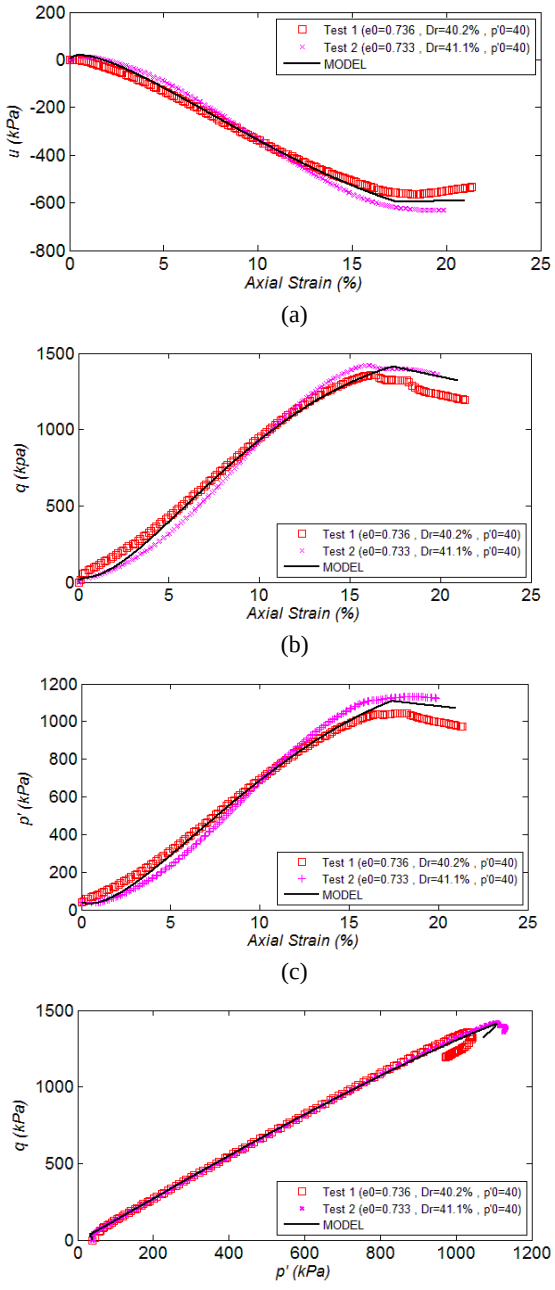

(a)

(b)

(c)

(d)

Fig. 6: The comparison of behavioral curves of Nevada sand in undrained experiment number 1 and 2 and behavioral model.
(a) *u:*ε_1 **(b)** *q:*ε_1 **(c)** *p':*ε_1 **(d)** *q:p'*

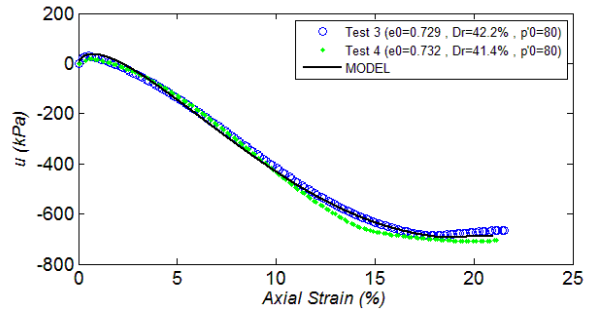

(a)

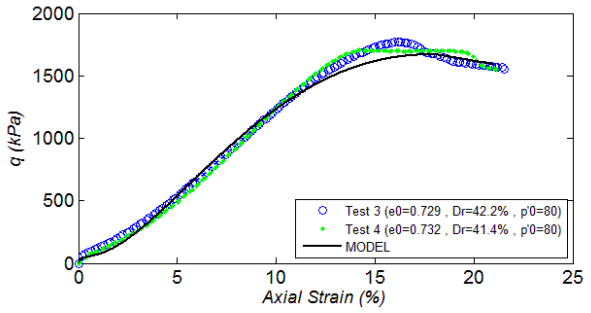

(b)

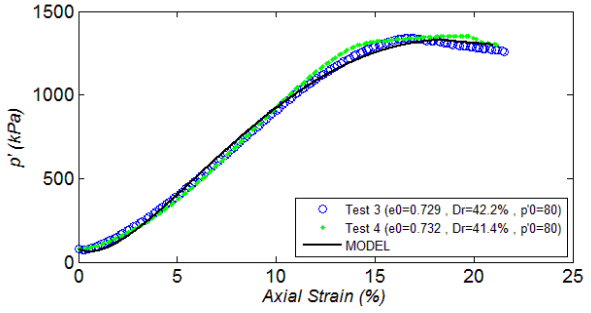

(c)

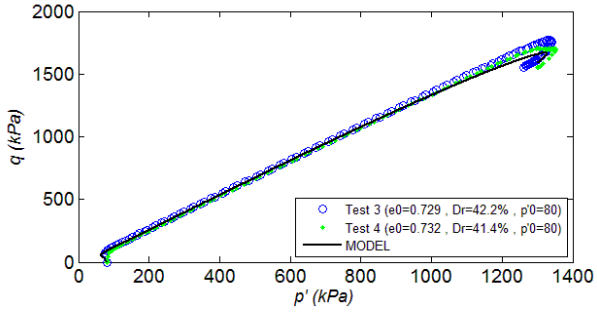

(d)

Fig. 7: The comparison of behavioral curves of Nevada sand in undrained experiment number 3 and 4 and behavioral model.
(a) u:ε_1
(b) q:ε_1
(c) p':ε_1
(d) q:p'

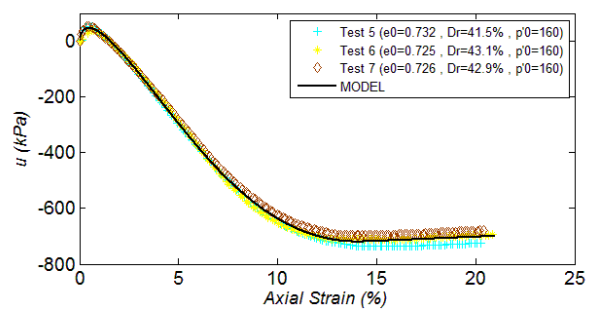

(a)

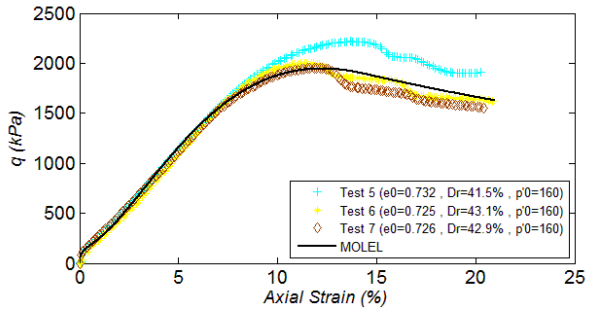

(b)

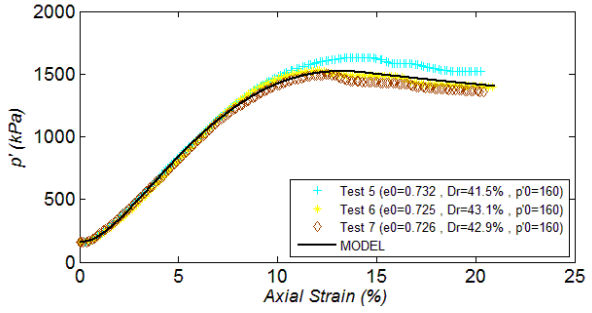

(c)

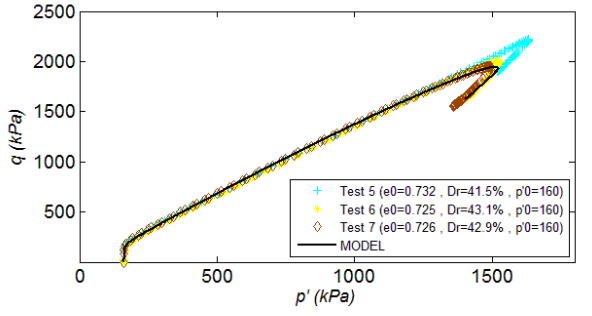

(d)

Fig. 8: The comparison of behavioral curves of Nevada sand in undrained experiment number 5, 6 and 7 and behavioral model.
(a) u:ε_1
(b) q:ε_1
(c) p':ε_1
(d) q:p'

[DOR: 20.1001.1.23454296.2017.2.1.5.4]
[DOI: 10.29252/nmce.2.1.49]

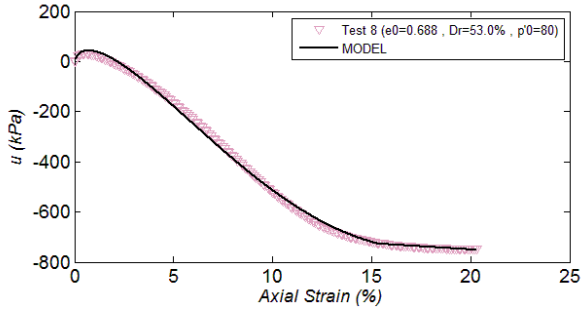

(a)

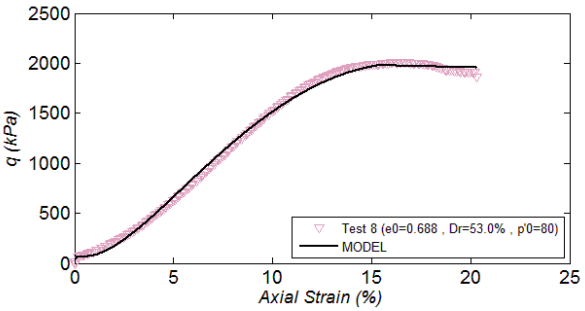

(b)

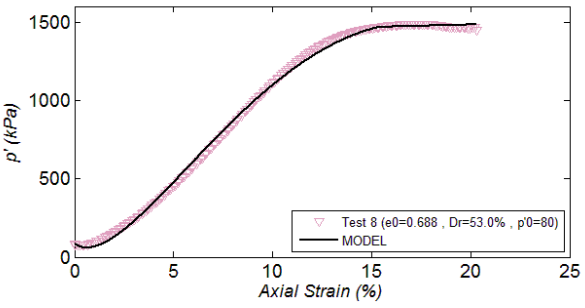

(c)

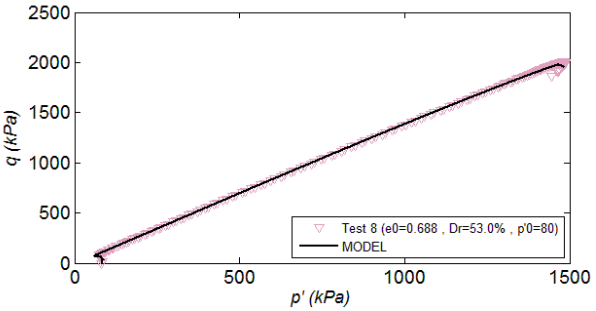

(d)

Fig. 9: The comparison of behavioral curves of Nevada sand in undrained experiment number 8 and behavioral model.
(a) u:ε_1
(b) q:ε_1
(c) p':ε_1
(d) q:p'

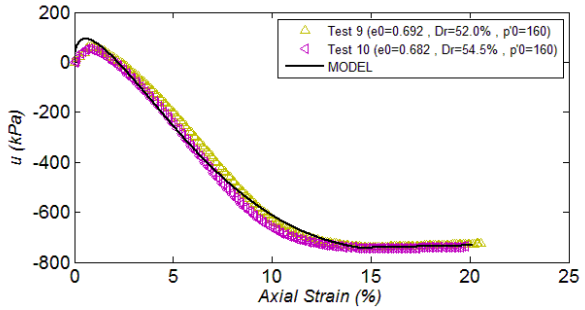

(a)

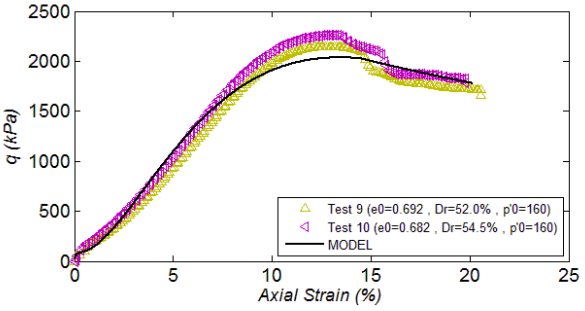

(b)

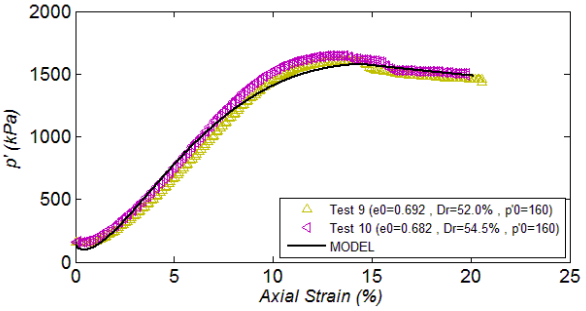

(c)

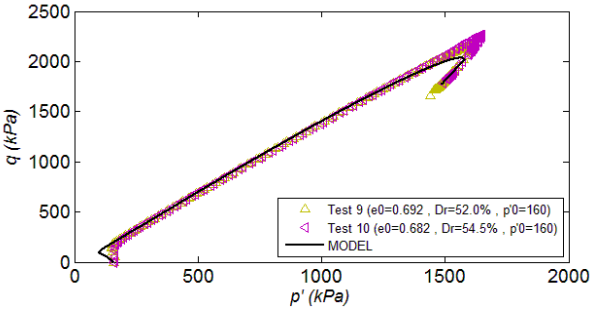

(d)

Fig. 10: The comparison of behavioral curves of Nevada sand in undrained experiment number 9 and 10 and behavioral model.
(a) u:ε_1
(b) q:ε_1
(c) p':ε_1
(d) q:p'

[DOR: 20.1001.1.23454296.2017.2.1.5.4]
[DOI: 10.29252/nmce.2.1.49]

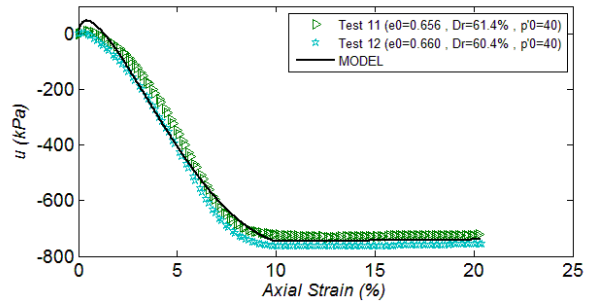

(a)

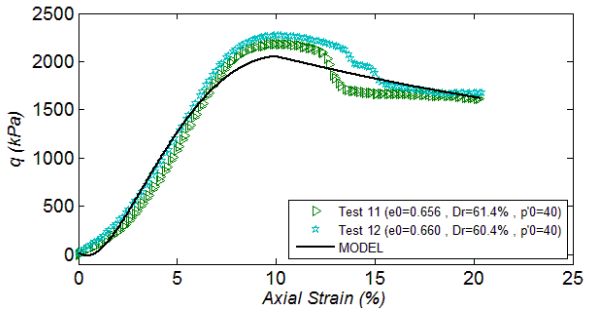

(b)

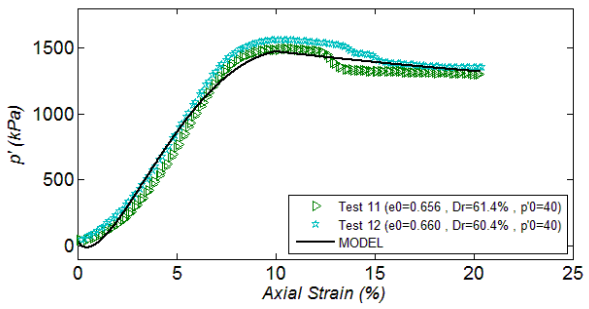

(c)

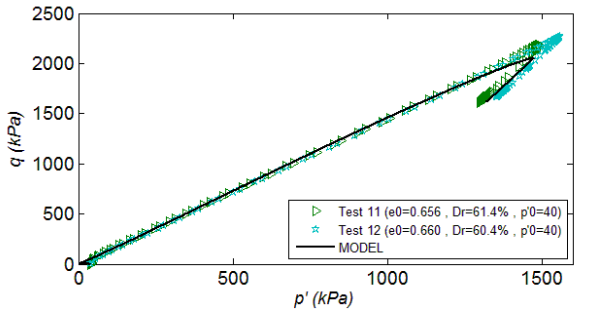

(d)

Fig. 11: The comparison of behavioral curves of Nevada sand in undrained experiment number 11 and 12 and behavioral model.
(a) u:ε_1
(b) q:ε_1
(c) p':ε_1
(d) q:p'

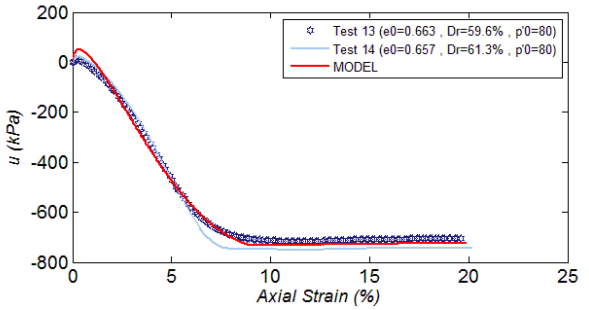

(a)

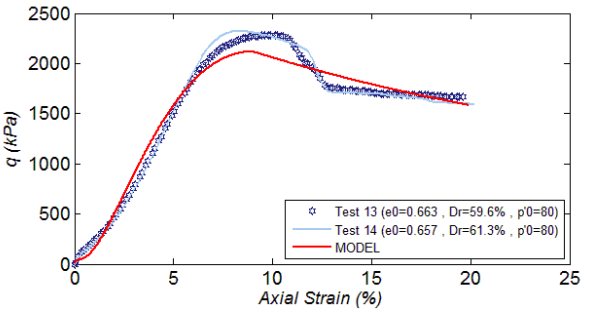

(b)

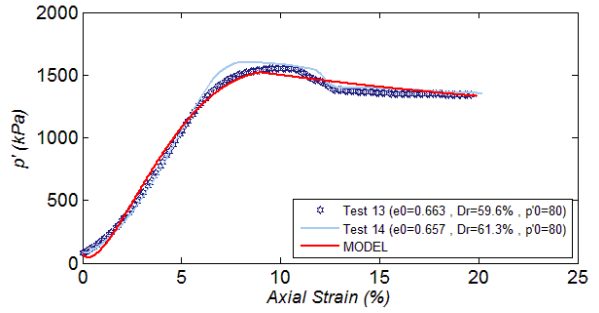

(c)

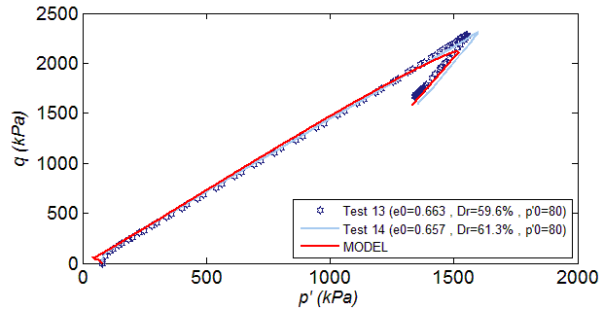

(d)

Fig. 12: The comparison of behavioral curves of Nevada sand in undrained experiment number 13 and 14 and behavioral model.
(a) u:ε_1
(b) q:ε_1
(c) p':ε_1
(d) q:p'

[DOR: 20.1001.1.23454296.2017.2.1.5.4]
[DOI: 10.29252/nmce.2.1.49]

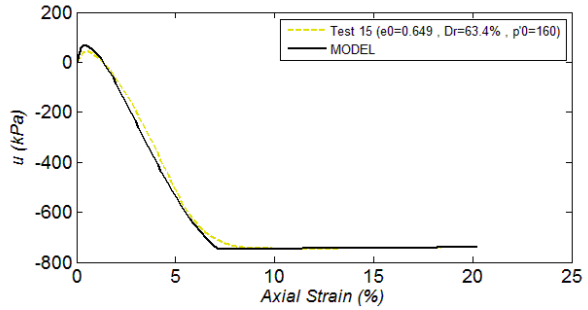

(a)

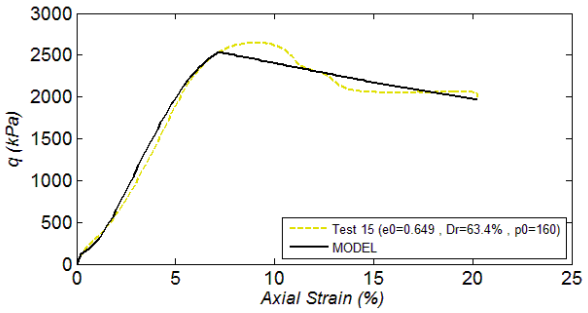

(b)

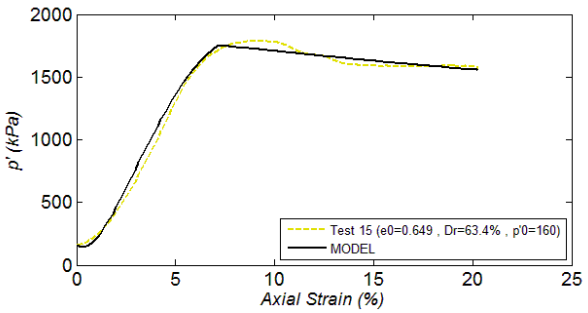

(c)

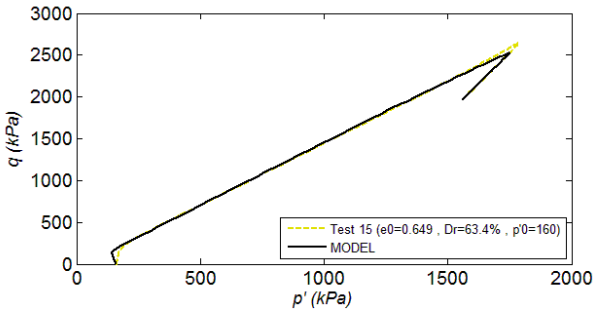

(d)

Fig. 13: The comparison of behavioral curves of Nevada sand in undrained experiment number 15 and behavioral model.
(a) u:ε_1
(b) q:ε_1
(c) p':ε_1
(d) q:p'

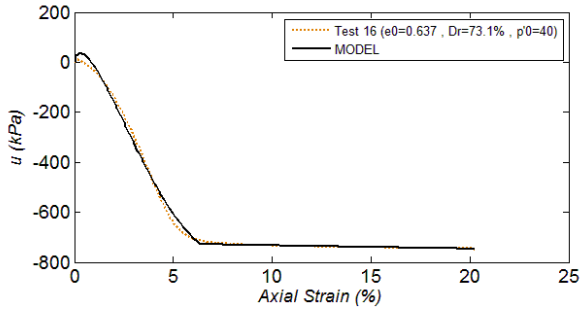

(a)

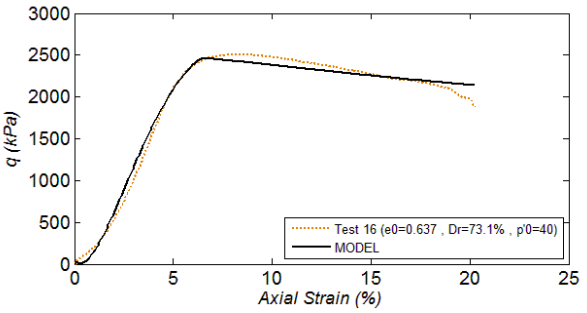

(b)

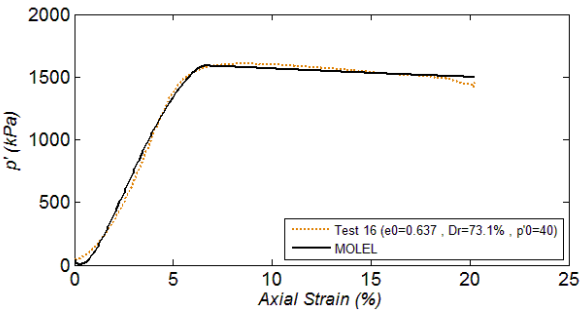

(c)

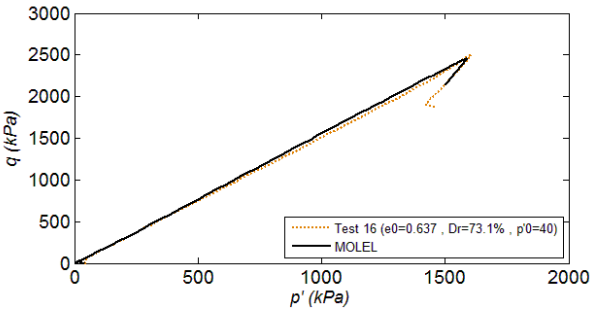

(d)

Fig. 14: The comparison of behavioral curves of Nevada sand in undrained experiment number 16 and behavioral model.
(a) u:ε_1
(b) q:ε_1
(c) p':ε_1
(d) q:p'

[DOR: 20.1001.1.23454296.2017.2.1.5.4]
[DOI: 10.29252/nmce.2.1.49]

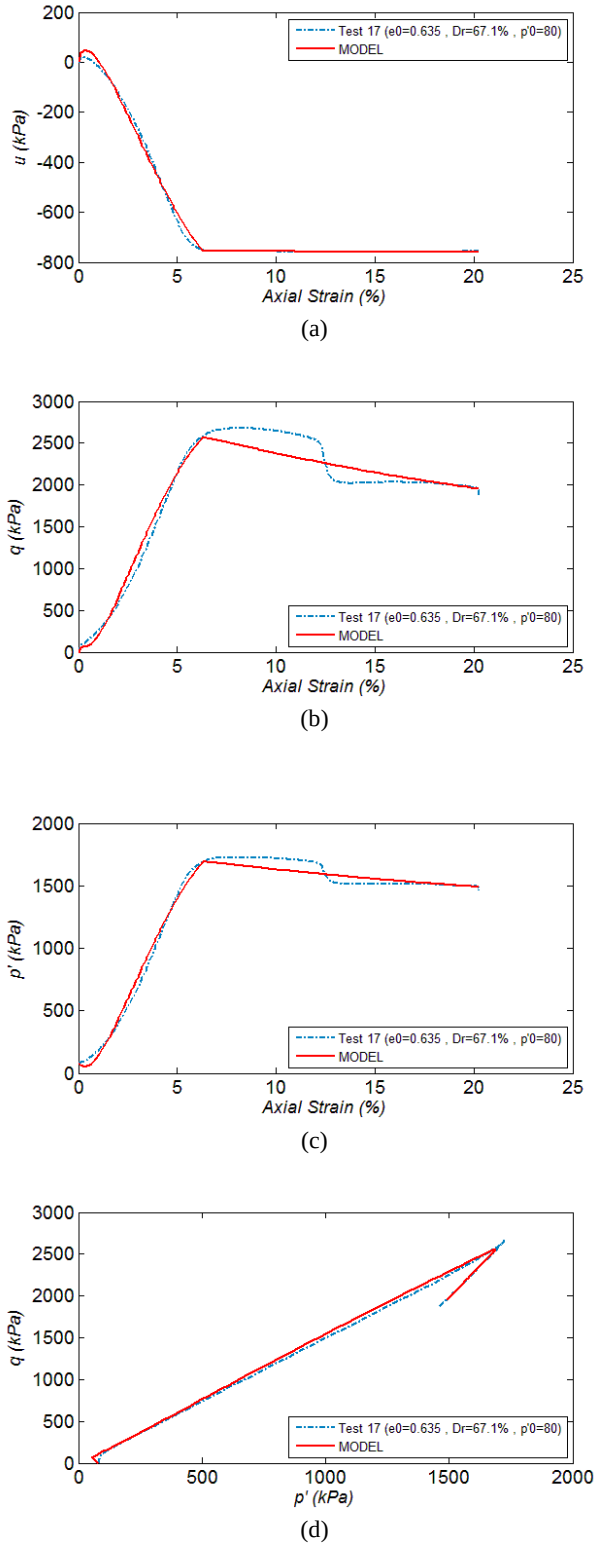

Fig. 15: The comparison of behavioral curves of Nevada sand in undrained experiment number 17 and behavioral model.

(a) u:ε_1

(b) q:ε_1

(c) p':ε_1

(d) q:p'

4. Conclusions

A parametric based hypo-elastic model simplifying the complexities in sand behavior proved capable of being used in engineering works. The required parameter was found based on the test results of triaxial standard tests. The capability of this hypo-elastic model is shown in predicting drained/undrained sample behavior with relatively high accuracy.

The required 11 parameters to evaluate material behavior in both drained and undrained conditions achieved despite short computer CPU times is quite impressive and admirable.

According to the proposed model formulation for undrained case, the presented pore water pressure equation is totally capable of calculating water pressure as a function of ε_{1i} which stands for the mathematical effects of hypo-elastic axial strain and a few constants which depend on volumetric changes in drained case. This relation reveals that the developed pore water pressure value at each stress increment depends on stress path and also the volumetric strain of sand skeleton against water bulk modulus shows that considering water compressibility that leads to a zero total volumetric strain of undrained sample.

The comparison of several test results with the model results shows the consistency of model in predicting soil behavior in drained and undrained cases.

Finally, the accuracy of predicted results is appreciable and shows the capability of this simple and quick model.

References:

[1] Arulanandan, K., Manzari, M., Zeng, X., Fagan, M., Scott, R.F. and Tan, T.S., 1995. Significance of the VELACS project to the solution of boundary value problems in geotechnical engineering.

[2] Arulmori, K., Muraleetharan, K. K., Hossain, M. M., and Fruth, L.S. (1992). VELACS laboratory Testing program, Soil Data Rep., Earth Technology Corporation, Irvine, Calif.

[3] Atkinson, J.H. and Bransby, P.L., 1977. The mechanics of soils, An introduction to critical state soil mechanics (No. Monograph).

[4] Been, K., 1999. The critical state line and its application to soil liquefaction. Physics and.

[5] Ishihara, K., 1996. Soil behaviour in earthquake geotechnics. Clarendon Press.

[6] Lee, K.L. and Seed, H.B., 1967. Drained strength characteristics of sands. Journal of Soil Mechanics & Foundations Div.

[7] Li, X.S. and Dafalias, Y.F., 2000. Dilatancy for cohesionless soils. Geotechnique, 50(4), pp.449-460.

[8] Ling, H.I. and Yang, S., 2006. Unified sand model based on the critical state and generalized plasticity. Journal of Engineering Mechanics, 132(12), pp.1380-1391.

[9] Manzari, M.T. and Dafalias, Y.F., 1997. A critical state two-surface plasticity model for sands. Geotechnique, 47(2), pp.255-272.

[10] Monkul, M.M. and Yamamuro, J.A., 2011. Influence of silt size and content on liquefaction behavior of sands. Canadian Geotechnical Journal, 48(6), pp.931-942.

[11] Monkul, M.M., 2010. Influence of silt size and content on static liquefaction potential of sand. Oregon State University.

[DOR: 20.1001.1.23454296.2017.2.1.5.4]

[DOI: 10.29252/nmce.2.1.49]

[12] Nova, R. and Wood, D.M., 1979. A constitutive model for sand in triaxial compression. International Journal for Numerical and Analytical Methods in Geomechanics, 3(3), pp.255-278.
[13] Olivera Bonilla, R.R., 2004. Numerical simulations of undrained granular media.
[14] Paster, M., Zienkiewicz, O.C. and Chan, A.H.C., 1990. Generalized plasticity and the modeling of soil behavior [J]. International Journal for Numerical and Analytical Methods in Geomechanics, 14(3), pp.151-190.
[15] RAHMAN, Z., Toll, D.G., Gallipoli, D. and Taha, M.R., 2010. Micro-structure and engineering behaviour of weakly bonded soil. Sains Malaysiana, 39(6), pp.989-997.
[16] Roscoe, K.H., Schofield, A. and Wroth, C.P., 1958. On the yielding of soils. Geotechnique, 8(1), pp.22-53.
[17] Sasiharan, N., 2006. Mechanics of dilatancy and its application to liquefaction problems (Vol. 68, No. 02).
[18] Shahir, H., Pak, A., Taiebat, M. and Jeremić, B., 2012. Evaluation of variation of permeability in liquefiable soil under earthquake loading. Computers and Geotechnics, 40, pp.74-88.
[19] Vaid, Y.P., Chung, E.K.F. and Kuerbis, R.H., 1990. Stress path and steady state. Canadian Geotechnical Journal, 27(1), pp.1-7.
[20] Verdugo, R. and Ishihara, K., 1996. The steady state of sandy soils. Soils and foundations, 36(2), pp.81-91.
[21] Wan, R.G. and Guo, P.J., 2001. Effect of microstructure on undrained behaviour of sands. Canadian Geotechnical Journal, 38(1), pp.16-28.
[22] Yin, Z.Y., Zhao, J. and Hicher, P.Y., 2014. A micromechanics-based model for sand-silt mixtures. International Journal of Solids and Structures, 51(6), pp.1350-1363.
[23] Zienkiewicz, O.C., 1984. Generalized plasticity formulation and application to geomechanics. Mech. Eng. Materials, pp.655-679.

[DOR: 20.1001.1.23454296.2017.2.1.5.4]
[DOI: 10.29252/nmce.2.1.49]